



Structural evolution during nanostructuring of additive manufactured 316L stainless steel by high-pressure torsion

Jae-Kyung Han^a, Xiaojing Liu^{b,c}, Isshu Lee^a, Yulia O. Kuzminova^d, Stanislav A. Evlashin^d, Klaus-Dieter Liss^{b,c}, Megumi Kawasaki^{a,*}

^a School of Mechanical, Industrial and Manufacturing Engineering, Oregon State University, Corvallis, OR 97331, USA

^b Materials and Engineering Science Program, Guangdong Technion - Israel Institute of Technology, Shantou, Guangdong 515063, China

^c Technion - Israel Institute of Technology, Haifa 32000, Israel

^d Center for Design, Manufacturing & Materials, Skolkovo Institute of Science and Technology, Moscow 121205, Russia

ARTICLE INFO

Keywords:

Defects
Microstructure
Nanocrystalline materials
Phase transformation
X-ray techniques

ABSTRACT

This study investigates the structural evolution including crystallite size, micro-strain, and lattice parameters of an additive manufactured 316L stainless steel during post-printing nanostructuring by high-pressure torsion (HPT) at room temperature. Formation of a martensite phase was observed in the nanostructured austenitic steel having an average grain size of 60 nm after 8 HPT turns. Significant strain gradients exist between the close-packed planes and out-of-close-packed-planes in the nanocrystalline structure, while such strain gradient was not observed in the as-built material. Structural changes occur in a very early stage of nanostructuring through 1/2 HPT turn and are attributed to severe lattice distortion by the excess of dislocations and defects.

1. Introduction

The 316L austenitic stainless steels (SS) have been well studied due to their good corrosion properties, high creep resistance and good formability. Nanostructuring by high-pressure torsion (HPT) was applied often for improving the mechanical properties of the steels [1,2]. Metal additive manufacturing (AM) is an influential subject among the recent materials science challenges, while a limited report focuses on strengthening of the AM steel [3]. Thus, the present report was initiated to examine the structural evolution of AM 316L SS during post-printing nanostructuring by applying transmission electron microscope (TEM) and X-ray diffraction (XRD) analyses.

2. Experimental

A bulk specimen was built with using Höganäs AM 316L SS powder having powder sizes of 20–53 μm. An AM technique of powder bed fusion was applied with a metal 3D printer, TRUMPF TruPrint 1000. The Chess X-Y scan strategy [4] was utilized with a square side of 4.0 mm in Ar atmosphere with a gas speed of 2.5 m/s, and other printing parameters are as follows: laser power of 113 W, laser speed of 700 mm/s, laser spot diameters of 55 μm, layer thicknesses of 20 μm, and hatch spacing

of 80 μm. An as-built 316L SS bar was machined to a shape of disk with 10 mm diameter and ~ 0.83 mm thickness, and these disks were processed by HPT under 6.0 GPa for 1/2, 1, 2, 4 and 8 turns at room temperature (24 ± 1 °C) and 1 rpm. The refined microstructure after 8 HPT turns was examined by a TEM, JEOL JEM-2100, and variation of hardness was examined by a Vickers microhardness tester, Mitutoyo HM-200, on well-polished sample surfaces. Evolution in structural characteristics was evaluated by XRD analysis employing a Rigaku SmartLab using Cu Kα radiation on the polished disk surfaces.

3. Results and discussion

An earlier report demonstrated unique microstructures of the 316L SS built through the Chess printing strategy [5]. It allows fast cooling leading to the formation of fine-grained microstructure having a sub-grain size of 300 nm in the as-built sample. HPT processing demonstrated further grain refinement, thus hardness improvements, across the disk diameters of the as-printed disks. In practice, variation in Vickers microhardness demonstrated that an initial hardness of $H_V = 233$ in the as-built condition increased to ~ 500 over the disk diameter after 8 HPT turns (see [Supplementary Fig. S1](#)).

[Fig. 1](#) shows a bright-field TEM image having an extra photo

* Corresponding author.

E-mail address: megumi.kawasaki@oregonstate.edu (M. Kawasaki).

<https://doi.org/10.1016/j.matlet.2021.130364>

Received 12 June 2021; Received in revised form 22 June 2021; Accepted 27 June 2021

Available online 30 June 2021

0167-577X/© 2021 Elsevier B.V. All rights reserved.

enlarging a local region, and a corresponding selected-area electron diffractogram (SAED) of the AM 316L SS after 8 HPT turns. Equiaxed ultrafine grains with an average grain size of 60 nm are shown in the image taken at the mid radius of the disk. Large numbers of dislocations and deformation twins indicated by the arrows are visible around and within grains, respectively. The SAED patterns imply the presence of γ -austenite with face-centered cubic (*f.c.c.*) structure and a limited formation of ϵ -martensite with hexagonal-close packed (*h.c.p.*) structure. Its azimuth intensity distribution supports the ultrafine grain size. XRD analysis was conducted at the overall disk surfaces of the 316L SS in as-built and after HPT and the line profiles are displayed in Fig. 2. Only a primary phase with *f.c.c.* structure was detected in all sample conditions, thereby suggesting a limited content of ϵ -martensite (below an XRD detection limit of ~ 5 vol%). The unregarded martensite phase associated with the larger observation region for XRD analysis than microstructural analysis is consistent with earlier reports on conventionally manufactured 316L SS after HPT at room temperature [6] and the limited phase transformation is described as a common behavior in 316L SS at a nanostructuring temperature range of 20–450 °C [7]. Grade 316L SS shows a limited deformation-induced martensitic transformation ($\gamma \rightarrow \alpha'$) followed by reverse transformation ($\alpha' \rightarrow \gamma$) with increasing strain by HPT [8], while a gradual martensitic transformation of $\gamma \rightarrow \epsilon \rightarrow \alpha'$ can be captured when the examined regions are localized [9]. Significant peak broadening is visible in each major *f.c.c.* peak of the AM 316L SS, which implies the refined crystallite sizes during nanostructuring. The relative peak intensities tend to show a strong {111} texture after HPT.

XRD analysis by a Williamson-Hall method was conducted and a plot of the full width at half maximum (FWHM), ΔQ , of the diffraction peaks against the scattering vector, Q , is shown in Fig. 3 for estimating crystallite sizes and micro-strain of the alloy in as-built and after HPT. Moreover, lattice parameters of the materials are computed based on the peak positions for all five *f.c.c.* plane coordinates. The changes in the structural parameters are summarized in Fig. 4 and the numerical data is available in Supplementary Table S1.

The construction of the Williamson-Hall plot revealed important structural changes by nanostructuring of the AM 316L SS. A closer look at Fig. 2 shows larger peak broadening at the out-of-close-packed-plane

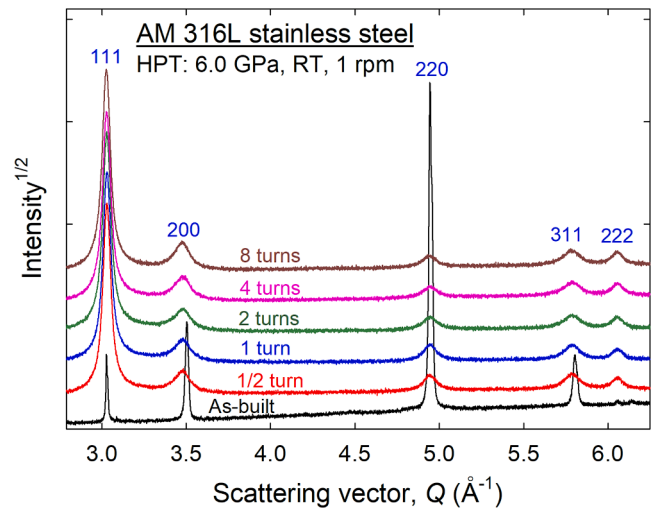


Fig. 2. XRD patterns of 316L SS in as-built and after HPT.

coordinates of 200, 220 and 311 that yield smaller coherent crystallite sizes than the coherent crystallite sizes obtained from the close-packed family planes of 111 and 222. Such inconsistency leads to a large scatter in ΔQ , thereby revealing significant strain gradients involving large numbers of defects within the crystalline structure introduced during HPT. The linear fitted lines for the nanostructured material were obtained by selecting only the close-packed family plane coordinates, while all four planes of 111, 200, 220, and 311 are considered for the as-built sample implying low defect density and strain in the structure. The consistent trend of large strain gradients within the nanocrystalline structure was observed in a nanostructured AM CoCrFeNi alloy [10], and it is comprehensible because of the similarity in the major alloying elements and the primary *f.c.c.* structure.

The obtained crystallite sizes and micro-strains show convincing structural evolution during nanostructuring of the steel. A significant increase in micro-strain after 1/2 HPT turn reduces the crystallite size

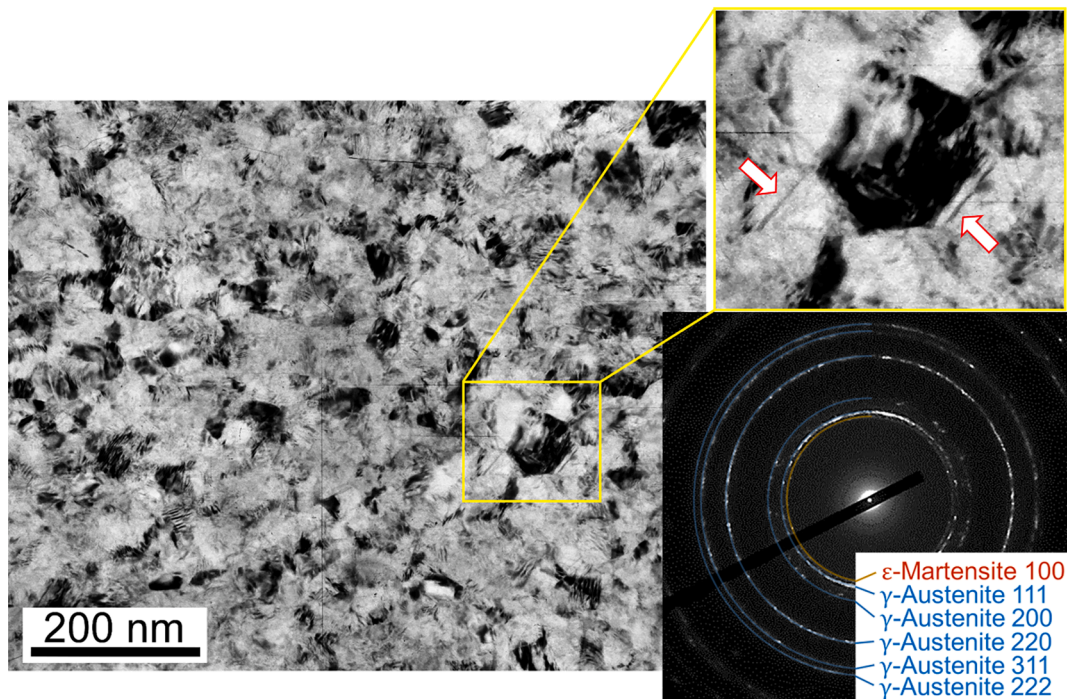


Fig. 1. TEM micrograph with an enlarged view showing twins and an SAED pattern of AM 316L SS after 8 HPT turns.

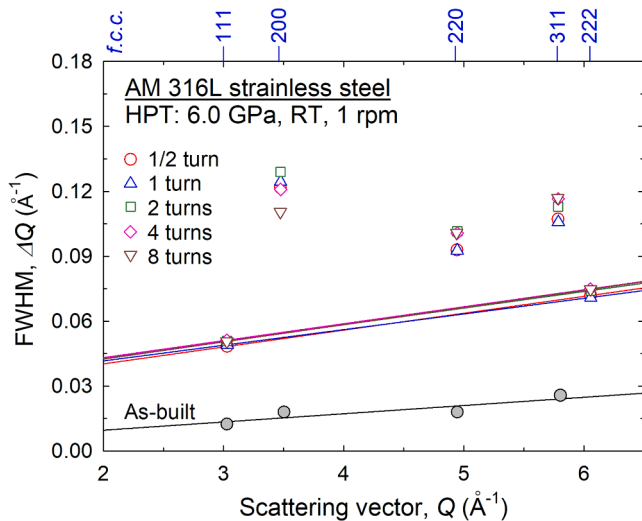


Fig. 3. A Williamson-Hall plot for the 316L SS in as-built and after HPT.

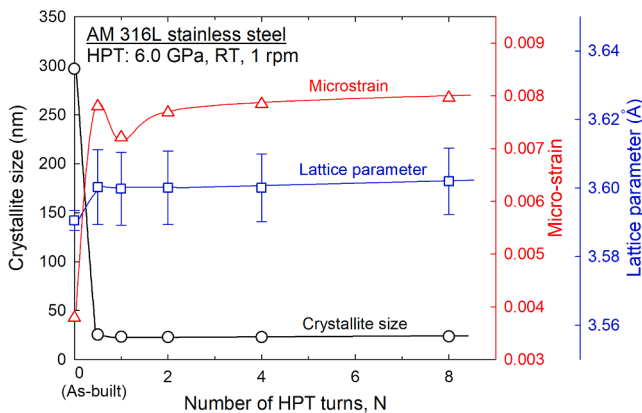


Fig. 4. Changes in coherent crystallite size, micro-strain and lattice parameter of 316L SS with HPT turns.

from 300 nm after printing, which agrees with the reported value [5], to 25 nm that is maintained consistent with increasing straining. The smaller crystallite size than the observed grain size of 60 nm by TEM implies a high density of dislocation walls forming cell structures in the refined microstructure. The lattice parameter increases by 0.27% during the first 1/2 turn and ultimately by 0.32% through 8 turns. Such increase in lattice parameter by nanostructuring towards 25 nm crystallite size is in good agreement with a report showing the inherent relationship of the lattice parameter increases by 0.1–0.3% during grain refinement to grain/crystallite sizes of 25–60 nm in various *f.c.c.* metal elements [11]. It is attributed to the crystal lattice distortion by the excess volume of dislocations, grain boundaries and other defects during severe nanostructuring, while the large error bars of the lattice parameters in the present steel are due to strain gradients, thus anisotropy, within crystals after HPT as described earlier.

4. Conclusions

Significant structural changes were demonstrated in an AM 316L SS during post-printing nanostructuring by HPT. XRD analysis revealed large strain gradients within the crystal structure, while the convincing

structural changes including a drastic decrease in crystallite size associated with a large increase in micro-strain were observed as early as 1/2 HPT turn. These changes and the lattice parameters increase by ~0.27–0.32% are attributed to the lattice distortion by the excess number of dislocations during nanostructuring of the AM 316L SS.

CRediT authorship contribution statement

Jae-Kyung Han: Investigation, Formal analysis. **Xiaoqing Liu:** Investigation, Formal analysis. **Isshu Lee:** Investigation, Formal analysis. **Yulia O. Kuzminova:** Resources, Investigation. **Stanislav A. Evlashin:** Resources. **Klaus-Dieter Liss:** Writing - review & editing. **Megumi Kawasaki:** Supervision, Writing - original draft.

Declaration of Competing Interest

The authors declare that they have no known competing financial interests or personal relationships that could have appeared to influence the work reported in this paper.

Acknowledgements

This study was supported by the National Science Foundation of the United States under Grant No. DMR-1810343.

Appendix A. Supplementary data

Supplementary data to this article can be found online at <https://doi.org/10.1016/j.matlet.2021.130364>.

References

- [1] H. Wang, I. Shuro, M. Umemoto, K. Ho-Hung, Y. Todaka, Annealing behavior of nano-crystalline austenitic SUS316L produced by HPT, *Mater. Sci. Eng. A* 556 (2012) 906–910.
- [2] S. Shi, Z. Zhang, X. Wang, G. Zhou, G. Xie, D.a. Wang, X.u. Chen, K. Ameyama, Microstructure evolution and enhanced mechanical properties in SUS316LN steel processed by high pressure torsion at room temperature, *Mater. Sci. Eng. A* 711 (2018) 476–483.
- [3] S.M. Yusuf, Y. Chen, S. Yang, N. Gao, Microstructural evolution and strengthening of selective laser melted 316L stainless steel processed by high-pressure torsion, *Mater. Charact.* 159 (2020), 110012.
- [4] A.M. Filimonov, O.A. Rogozin, D.G. Firsov, Y.O. Kuzminova, S.N. Sergeev, A. P. Zhilyaev, M.I. Lerner, N.E. Toropkov, A.P. Simonov, I.I. Binkov, I.V. Okulov, I. S. Akhatov, S.A. Evlashin, Hardening of additive manufactured 316L stainless steel by using bimodal powder containing nanoscale fraction, *Materials* 14 (2020) 115.
- [5] Y. Kuzminova, D. Firsov, S. Konev, A. Dudin, S. Dagesyan, I. Akhatov, S. Evlashin, Structure control of 316L stainless steel through an additive manufacturing, *Lett. Mater.* 9 (4s) (2019) 551–555.
- [6] S. Scheriau, Z. Zhang, S. Kleber, R. Pippan, Deformation mechanisms of a modified 316L austenitic steel subjected to high pressure torsion, *Mater. Sci. Eng. A* 528 (6) (2011) 2776–2786.
- [7] M.M. Abramova, N.A. Enikeev, R.Z. Valiev, A. Etienne, B. Radiguet, Y. Ivanisenko, X. Sauvage, Grain boundary segregation induced strengthening of an ultrafine-grained austenitic stainless steel, *Mater. Lett.* 136 (2014) 349–352.
- [8] Y. Mine, Z. Horita, Y. Murakami, Effect of hydrogen on martensite formation in austenitic stainless steels in high-pressure torsion, *Acta Mater.* 57 (10) (2009) 2993–3002.
- [9] J. Gubicza, M. El-Tahawy, Y.i. Huang, H. Choi, H. Choe, J.L. Lábár, T.G. Langdon, Microstructure, phase composition and hardness evolution in 316L stainless steel processed by high-pressure torsion, *Mater. Sci. Eng. A* 657 (2016) 215–223.
- [10] W. Zhao, J.-K. Han, Y.O. Kuzminova, S.A. Evlashin, A.P. Zhilyaev, A.M. Pesin, J.-I. Jang, K.-D. Liss, M. Kawasaki, Significance of grain refinement on micro-mechanical properties and structures of additively-manufactured CoCrFeNi high-entropy alloy, *Mater. Sci. Eng. A* 807 (2021), 140898.
- [11] W. Qin, T. Nagase, Y. Umakoshi, J.A. Szpunar, Relationship between microstrain and lattice parameter change in nanocrystalline materials, *Philos. Mag. Lett.* 88 (3) (2008) 169–179.